Infectious Diseases and Immunology
Publications

Infectious Diseases and Immunology

Type I Interferon Transcriptional Signature in Neutrophils and Low-Density Granulocytes Are Associated with Tissue Damage in Malaria

Bruno Coelho Rocha
Universidade Federal de Minas Gerais

Et al.

Let us know how access to this document benefits you.

Repository Citation

Cell Reports

Type I Interferon Transcriptional Signature in Neutrophils and Low-Density Granulocytes Are Associated with Tissue Damage in Malaria

Graphical Abstract
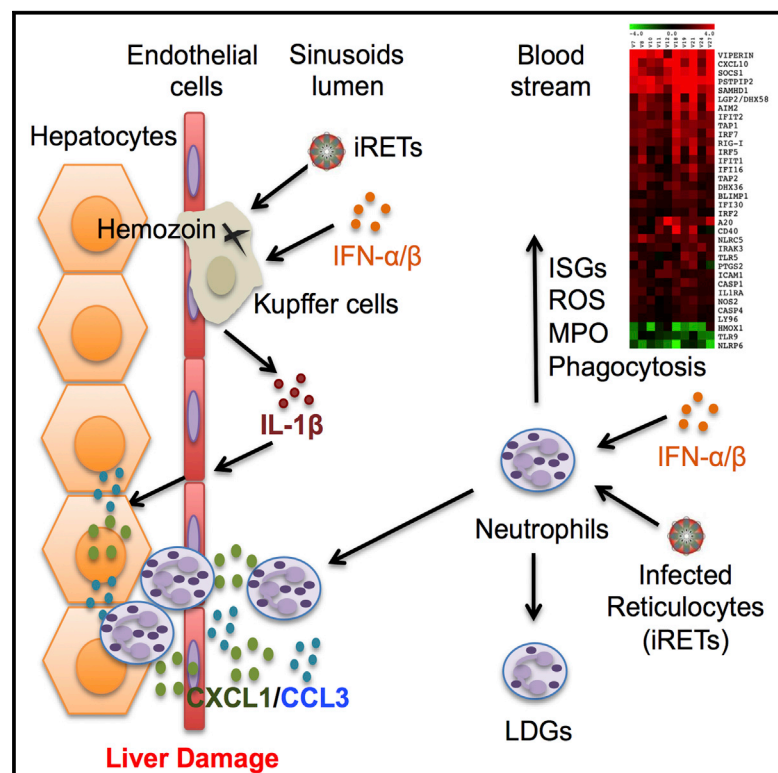
Authors

Bruno Coelho Rocha,
Pedro Elias Marques,
Fabiana Maria de Souza Leoratti, ...,
Gustavo Batista Menezes,
Douglas Taylor Golenbock,
Ricardo Tostes Gazzinelli

Correspondence

douglas.golenbock@umassmed.edu
(D.T.G.),
ritoga@cpqrr.fiocruz.br (R.T.G.)

In Brief

Rocha et al. demonstrate an increased frequency of activated neutrophils and low-density granulocytes in *P. vivax* patients. The activation stage of neutrophils was associated with a type I IFN transcriptional signature. Importantly, IFNAR and caspase 1/11 were shown to play a central role in neutrophil recruitment and liver damage in rodent malaria.

Highlights

- Neutrophils are highly activated during *P. vivax* infection

- *P. vivax* infection induces a high frequency of low-density granulocytes

- Neutrophils from malaria patients display a type I IFN transcriptional signature

- IFNAR and caspase 1 induce neutrophil recruitment and liver damage in rodent malaria

CellPress

Type I Interferon Transcriptional Signature in Neutrophils and Low-Density Granulocytes Are Associated with Tissue Damage in Malaria

Bruno Coelho Rocha,[1,2,3] Pedro Elias Marques,[4] Fabiana Maria de Souza Leoratti,[3] Caroline Junqueira,[3] Dhelio Batista Pereira,[5] Lis Ribeiro do Valle Antonelli,[3] Gustavo Batista Menezes,[4] Douglas Taylor Golenbock,[2,6,*] and Ricardo Tostes Gazzinelli[1,2,3,6,*]

[1]Departamento de Bioquímica e Imunologia, Instituto de Ciências Biológicas, Universidade Federal de Minas Gerais, Belo Horizonte 31270-901, Brazil
[2]Department of Medicine, University of Massachusetts Medical School, Worcester, MA 01605, USA
[3]Centro de Pesquisas Rene Rachou, Fundação Oswaldo Cruz–Minas Gerais, Belo Horizonte 30190-002, Brazil
[4]Departamento de Morfologia, ICB, Universidade Federal de Minas Gerais, Belo Horizonte 31270-901, Brazil
[5]Centro de Pesquisas em Medicina Tropical, Fundação Oswaldo Cruz–Rondônia, Porto Velho 76812-329, Brazil
[6]Co-senior author
*Correspondence: douglas.golenbock@umassmed.edu (D.T.G.), ritoga@cpqrr.fiocruz.br (R.T.G.)
http://dx.doi.org/10.1016/j.celrep.2015.11.055

SUMMARY

Neutrophils are the most abundant leukocyte population in the bloodstream, the primary compartment of *Plasmodium* sp. infection. However, the role of these polymorphonuclear cells in mediating either the resistance or the pathogenesis of malaria is poorly understood. We report that circulating neutrophils from malaria patients are highly activated, as indicated by a strong type I interferon transcriptional signature, increased expression of surface activation markers, enhanced release of reactive oxygen species and myeloperoxidase, and a high frequency of low-density granulocytes. The activation of neutrophils was associated with increased levels of serum alanine and aspartate aminotransferases, indicating liver damage. In a rodent malaria model, we observed intense recruitment of neutrophils to liver sinusoids. Neutrophil migration and IL-1β and chemokine expression as well as liver damage were all dependent on type I interferon signaling. The data suggest that type I interferon signaling has a central role in neutrophil activation and malaria pathogenesis.

INTRODUCTION

Malaria infected approximately 200 million people in 2013, and an estimated 584,000 of these people died (World Health Organization, 2014). *Plasmodium vivax* is the most widespread human *Plasmodium* species and represents a major social and economic health problem, especially in Latin America and Asia (Mueller et al., 2009; World Health Organization, 2014). On the other hand, *Plasmodium falciparum* is more prevalent in Africa and is responsible for most of the deaths from malaria (World

Health Organization, 2014). Although the pathology associated with malaria occurs during the erythrocytic stage of infection, the liver is an important organ for malaria infection, because *Plasmodium* infects hepatocytes early in its life cycle, where it replicates asexually before reaching the blood stage (Prudêncio et al., 2006; Sturm et al., 2006). Furthermore, the liver is also an important organ for the trapping and clearance of *Plasmodium*-infected red blood cells (Krücken et al., 2009; Murthi et al., 2006). As a result, there is an intense recruitment of leukocytes to the liver during the acute phase of malaria (Haque et al., 2011).

The complexity of parasite-host interactions and the limited knowledge of the mechanisms by which *Plasmodium* spp. trigger innate immune cells are the main impediments in understanding the pathogenesis of malaria (Gazzinelli et al., 2014). Surprisingly, the role of neutrophils in malaria has rarely been addressed.

Neutrophils are polymorphonuclear leukocytes (PMNs) capable of eliminating bacterial and fungal infections by multiple mechanisms (Mantovani et al., 2011). In addition to being the primary effectors of the immune response against microbial pathogens, neutrophils are also central mediators of inflammatory injury. However, the role of neutrophils in host resistance and pathogenesis of malaria is still controversial. Nevertheless, an altered function of neutrophils has been reported in both *P. vivax* and *P. falciparum* malaria (Cunnington et al., 2012; Leoratti et al., 2012).

Type I interferons (IFNs) are cytokines that play an important role in the protection against viral infections. Type I interferons possess strong immunomodulatory activity. The production of type I IFNs has been associated with many other pathogens, including *Mycobacterium* (Antonelli et al., 2010), *Leishmania* (Xin et al., 2010), and *Plasmodium* (Aucan et al., 2003; Haque et al., 2014; Sharma et al., 2011). Type I IFNs modulate macrophages, monocytes, dendritic cells, and neutrophils through many different mechanisms (Salazar-Mather et al., 2002; Seo et al., 2011; Swiecki et al., 2011). Despite the high frequency of malaria, the roles of type I IFN in regulating neutrophils during
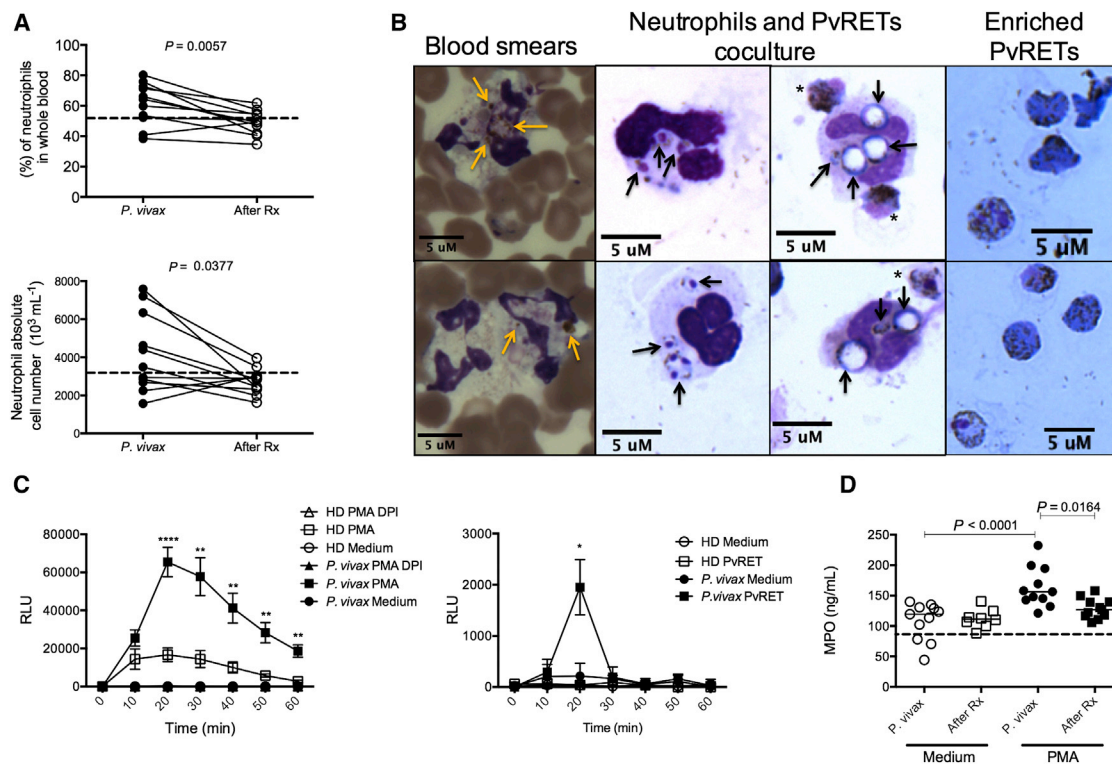
Figure 1. Neutrophils from *P. vivax*-Infected Patients Display a Highly Activated Phenotype

(A) Frequency (top) and absolute numbers (bottom) of neutrophils stained within whole blood from *P. vivax*-infected patients before and 30–45 days after treatment (After Rx). Each pair of circles connected by a line represents a single patient (n = 11). The absolute numbers were calculated based on their frequency and total leukocytes numbers. Dashed lines represent the median of given measurements for five healthy donors.

(B) Left: neutrophils containing hemozoin (yellow arrows) from *P. vivax*-infected patient blood smears. Center: parasite components and hemozoin in vacuoles (black arrows) of neutrophils after in vitro incubation with PvRETs (asterisks). Right: enriched PvRETs from peripheral blood of malaria patients by Percoll gradient.

(C) The kinetics of ROS production by neutrophils from patients with acute *P. vivax* infection or HDs cultured in medium alone or with 100 ng/ml PMA in the presence or absence of the ROS inhibitor DPI (5 μM) (n = 5–7) (left) or stimulated with purified PvRETs (neutrophil:PvRET ratio, 2:1) (n = 4) (right). Luminol was measured by chemiluminescence (relative light units [RLUs]) for 60 min. Data are represented as mean ± SEM. The differences are relative to HDs. *p < 0.05, **p < 0.01, ****p < 0.0001. Individual values of PMA- or PvRET-induced ROSs released by neutrophils from *P. vivax*-infected patients and HDs are depicted in Figure S2.

(D) MPO levels in supernatants of unstimulated and PMA-activated (100 ng/ml) neutrophils from *P. vivax*-infected patients before and after treatment for 24 hr (n = 11). Dashed lines represent the median of given measurements for five healthy donors.

See also Figures S1 and S2.

infection have not been explored. Therefore, we decided to focus on the importance of type I IFN in orchestrating neutrophil activation and function during malaria. We found that, in both human and rodent malaria, neutrophil activation by type I IFN is associated with increased levels of circulating transaminases, indicative of liver pathology. Furthermore, we found that type I IFN modulates caspase-1/11 activation, pro-interleukin 1β (pro-IL-1β), and chemokine mRNA expression as well as neutrophil migration to the livers of infected mice. Together, our results suggest that type I IFNs are responsible for neutrophil-mediated liver pathology during human and rodent malaria.

RESULTS

Neutrophils from *P. vivax*-Infected Patients Are Highly Activated

We observed an increase in the frequency and absolute number of neutrophils in the peripheral blood of *P. vivax*-infected pa-

tients (Figure 1A). To obtain these results, we used CD66b and CD15 as neutrophil markers. As shown in Figures S1A and S1B, more than 98% of neutrophils from malaria patients expressed both markers. We also observed a low frequency of neutrophils containing hemozoin in blood smears of *P. vivax*-infected patients (Figure 1B, left). The arrows in the center indicate parasites and hemozoin (Hz) inside neutrophil vacuoles after 30 min of in vitro incubation with *P. vivax*-infected reticulocytes (PvRETs). Preparations of enriched PvRETs are shown in Figure 1B (right). To evaluate their activation status, we assessed the kinetics of reactive oxygen species (ROS) production after stimulation with phorbol 12-myristate 13-acetate (PMA) and with PvRETs. Total ROS production was evaluated in purified neutrophils by luminol assay. Neutrophils from acutely infected patients produced significantly higher levels of ROS than neutrophils from healthy donors (HDs) when stimulated with PMA. These differences persisted over 1 hr of stimulation. Pre-treating cells with a nicotinamide adenine
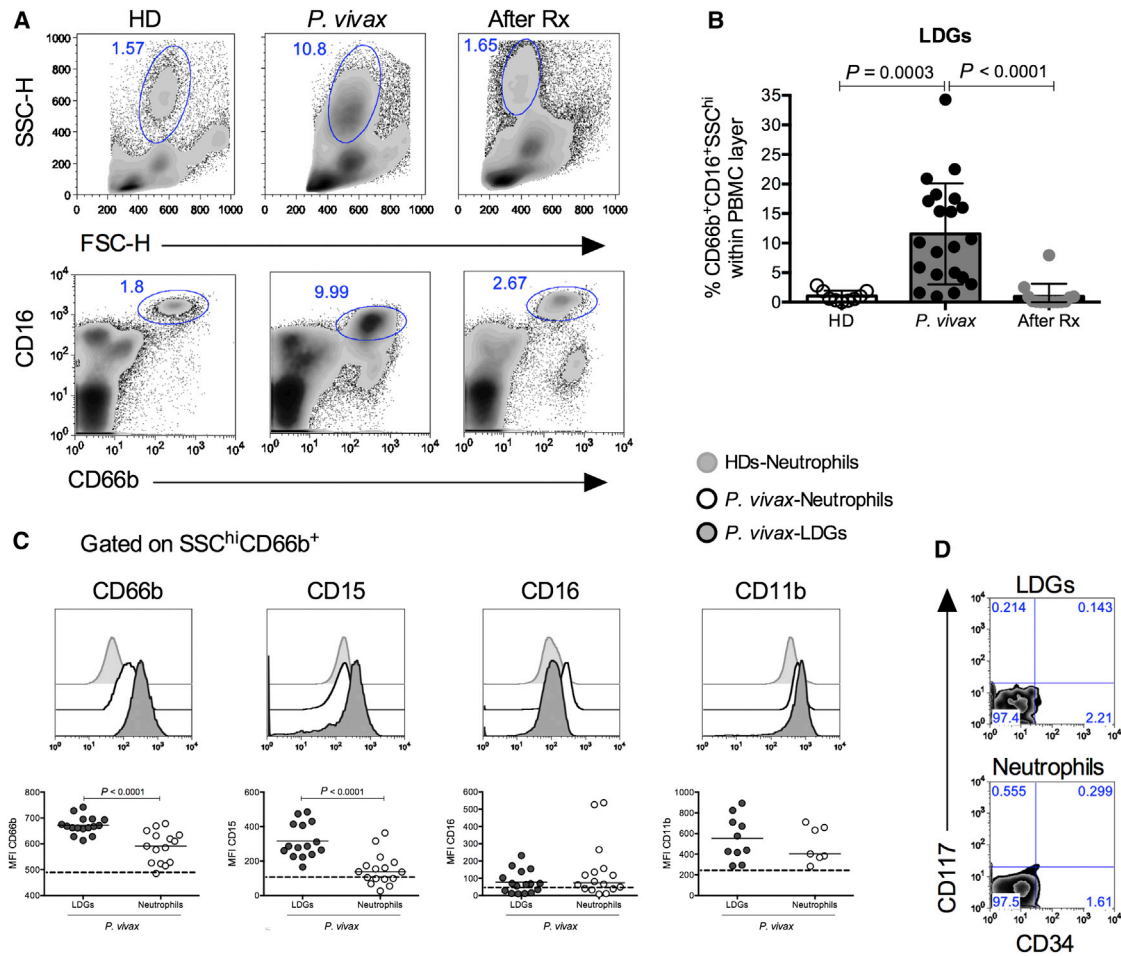
Figure 2. Low-Density Granulocytes Are Increased and Activated in PBMCs from Patients with Acute *P. vivax* Infections

(A and B) Representative density plots (A) and bar graph (B) indicating the frequencies of SSC^{hi}CD66b$^+$CD16$^+$ (LDGs) within PBMCs of HDs (white circles) (n = 9) and *P. vivax*-infected patients before (black circles, n = 21) and after treatment (gray circles, n = 14). Data are represented as mean ± SD. Numbers within or beside each box refer to the cell frequencies within each gate (A).

(C) Top: representative histograms of CD66b, CD15, CD16, and CD11b of LDGs and neutrophils from *P. vivax*-infected patients and neutrophils from HDs gated previously on SSC^{hi}CD66b$^+$. Light gray histogram, neutrophils from HDs; dark gray histogram, LDGs; white histogram, neutrophils from *P. vivax*-infected patients. Bottom: MFI scatterplots of the respective activation markers in LDGs (gray circles) and neutrophils (white circles) from *P. vivax*-infected patients and neutrophils from HDs (dashed line). Each circle represents one patient (n = 9–16). Numbers within or beside each box refer to the cell frequencies within each gate.

(D) Representative zebra plot of CD34 and CD117 cell frequencies in LDGs and neutrophils from *P. vivax*-infected patients. Numbers within or beside each box refer to the cell frequencies within each gate.

See also Figure S3.

dinucleotide phosphate (NADPH) oxidase inhibitor, diphenyleneiodonium chloride (DPI), completely abrogated ROS production in neutrophils from *P. vivax*-infected patients as well as in neutrophils from HDs. Similarly PvRETs also induced an augmented ROS production by neutrophils from *P. vivax*-infected patients (Figure 1C). We also measured myeloperoxidase (MPO) production by these cells after 24 hr of stimulation with PMA. Neutrophils from *P. vivax*-infected patients treated with PMA released significantly higher levels of MPO than neutrophils from the same patients after chemotherapy or neutrophils purified from HDs (Figure 1D). Together, these results indicate that neutrophils are highly activated and become hyper-responsive during *P. vivax* infection.

P. vivax Infection Induces an Increased Frequency of Activated Low-Density Granulocytes in the Peripheral Blood

Using conventional density gradient centrifugation to separate peripheral blood mononuclear cells (PBMCs) from malaria-infected patients, we found a higher frequency of a leukocyte subset with a high side scatter height (SSC-H) compared with those purified from healthy donors or cured patients (Figure 2A). We subsequently found that the frequency of SSC^{hi}CD66b$^+$CD16$^+$ cells within PBMCs was significantly higher in *P. vivax*-infected patients than in uninfected controls (Figure 2B). These cells did not express CD14 or major histocompatibility complex (MHC) class II molecules, confirming that they are not monocytes
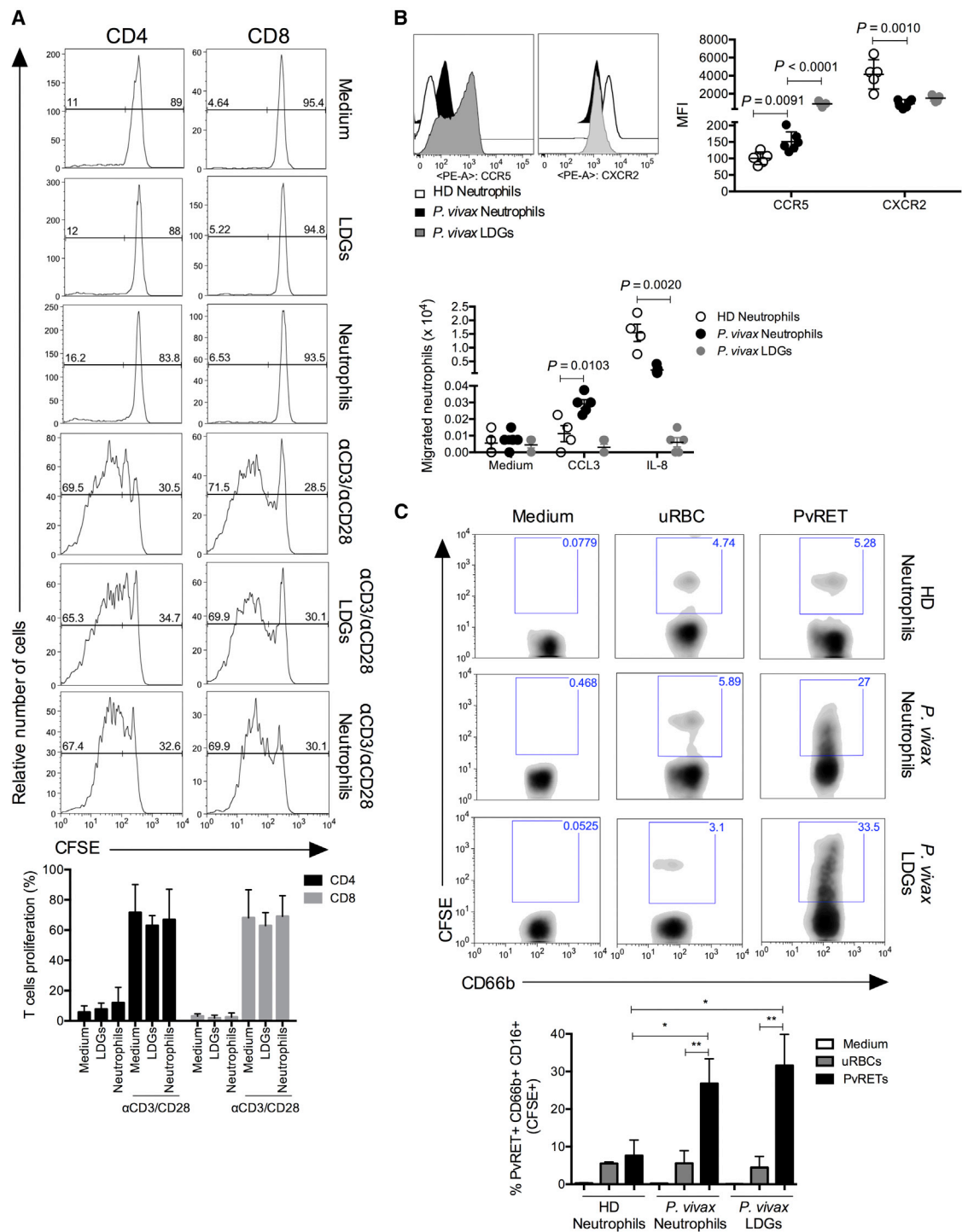
Figure 3. Functional Characterization of LDGs from *P. vivax*-Infected Patients

(A) Top: CFSE-labeled PBMCs from *P. vivax*-infected patients after LDG purification stimulated with soluble αCD3 (1 μg/ml) and αCD28 (0.5 μg/ml) in the presence or absence of LDGs or neutrophils (PBMC:LDG or neutrophil ratio, 2:1). After 4 days, CD4+ (left) and CD8+ (right) T cell proliferation was determined by flow cytometry after gating the CD3+ population and measuring the percentage of CFSE^low T cells. Bottom: percentage of CD4 and CD8 cell proliferation. Data are presented as mean ± SD (n = 5).

(Figure S3). Therefore, this leukocyte subset, which also expresses CD15, was defined as low-density granulocytes (LDGs) (Brandau et al., 2011; Denny et al., 2010).

We next investigated the expression of activation markers within LDGs and neutrophils from 16 malaria patients as well as neutrophils from HDs. We observed that the median fluorescence intensity (MFI) of CD15 and CD66b from LDGs of *P. vivax*-infected patients was significantly higher than the MFI of these markers on purified neutrophils. There was no observable difference in either CD16 or CD11b expression in LDGs versus PMNs (Figure 2C). CD34 and CD117, markers expressed on early progenitors, were not detected on either LDGs or neutrophils. Taken together, the profile of surface molecular expression suggests that LDGs are activated neutrophils that have degranulated during *P. vivax* infection.

We next performed functional assays to determine the relevance of LDGs in *P. vivax* infection. Because LDGs express surface markers similar to granulocytic/neutrophilic myeloid-derived suppressor cells (MDSCs) (Brandau et al., 2011; Rodriguez et al., 2009), we tested their ability to inhibit T cell proliferation. We found that neither LDGs nor neutrophils from *P. vivax*-infected patients suppressed T cell proliferation after stimulation with αCD3/αCD28 (Figure 3A). Furthermore, we showed that LDGs have an impaired migration toward CCL3 or IL-8 even though the expression of chemokines receptors was not reduced (Figure 3B). As we have shown previously, the migration to IL-8 was reduced in neutrophils from malaria patients (Leoratti et al., 2012). Interestingly, we observed that neutrophils from *P. vivax*-infected patients have an enhanced migration capacity to CCL3. This was associated with an increased expression of the chemokine receptor CCR5 (Figure 3B). Finally, we observed that LDGs have increased phagocytic activity, similar to neutrophils from malaria patients, compared with neutrophils from HDs (Figure 3C). Unexpectedly, we found low levels of phagocytosis of uninfected red blood cells (uRBCs) by LDGs as well as neutrophils from malaria patients and healthy donors. This background of our assay indicates low levels of internalization of carboxyfluorescein succinimidyl ester (CFSE)-labeled uRBCs that may have been damaged during the experimental procedure. Nevertheless, the difference of phagocytosis between uRBCs and PvRETs is dramatic and indicates that infected reticulocytes are indeed actively internalized by neutrophils and LDGs from *P. vivax*-infected patients.

Neutrophils Have an Interferon Transcriptional Signature during *P. vivax* Infection

We next profiled mRNA expression of highly enriched neutrophils (>99% purity; Figure S4A) collected from ten *P. vivax*-infected patients. We excluded the influence of significant monocyte contamination in these neutrophil preparations because we could not detect CD14+ cells in our preparation (Figure S4B). In

addition, we analyzed our preparations for cytokine transcripts, including *IFN-α* and *IFN-β* as well as chemokines that are produced by monocytes and not neutrophils, and they were not detected in this assay (Figure S4C). In agreement, different studies indicate that neutrophils do not produce type I IFN (von der Ohe et al., 2001; Yamaguchi et al., 1977). Furthermore, we assessed the mRNA and protein levels of IL-1β by neutrophils and monocytes from *P. vivax*-infected patients. Our results indicate that malaria infection does not induce an upregulation of neutrophil *IL-1β* transcripts and that these cells did not produce IL-1β after LPS challenge (Figure S4D). A custom codeset for nanostring analysis was designed, containing 98 genes related to inflammatory responses. Of 66 genes that were expressed by neutrophils, we found that 34 genes were differentially expressed upon *P. vivax* infection with a fold change of more than 1.8 and a p value of less than 0.05 compared with purified neutrophils from the same patients after chemotherapy (Table S1). Of these 34 differentially expressed genes, 19 were considered to be IFN-stimulated genes (ISGs) (Figure 4A).

To get a clearer idea of what constitutes a "type I IFN signature," we purified neutrophils from HDs and stimulated them with either type I IFN or type II IFN (IFN-γ). We observed that most of the ISGs highly induced during malaria were predominantly type I IFN-dependent, although IFN-γ also stimulated some of these genes but, generally, to a lesser extent (Figure 4B). We also investigated ISG transcriptional expression in LDGs from *P. vivax*-infected patients. ISG expression by LDGs was lower than by neutrophils, suggesting that these cell populations have different roles during malaria infection (Figure 4C). Finally, we observed a positive correlation between ISGs and aspartate (AST) serum levels in *P. vivax*-infected patients (Figure 4D). The malaria patients enrolled in this study had significantly increased levels of serum alanine (ALT) and AST aminotransferases compared with the same patients after therapy (Figure S4E). In summary, these data suggest that neutrophils from *P. vivax*-infected patients have a predominantly type I IFN transcriptional signature that correlates positively with liver damage.

Neutrophil Recruitment and Liver Damage in *Plasmodium chabaudi*-Infected Mice

Based on the hypothesis that neutrophils may be triggering liver damage during malaria, we investigated this phenomenon in mice infected with the blood stage of *P. chabaudi*. We first measured the recruitment of granulocytes on days 7, 11, and 14 post-infection by confocal intravital microscopy using anti-GR1 (Figure 5A). These results were confirmed by using the anti-Ly6G (clone 1A8) antibody, which is more specific for neutrophils (Movie S1). The success of infection was confirmed by blood smears and by the presence of pigment (hemozoin) found only in infected livers (Figure 5A). We counted an average of 25.73 ± 4.69 (mean ± SEM) neutrophils per 10× field in

---

(B) Top: histograms and MFI of CCR5 and CXCR2 expression in neutrophils (n = 6) and LDGs (n = 5) from *P. vivax*-infected patients and neutrophils from HDs (n = 5). Bottom: chemotaxis toward CCL3 (50 ng/ml) and IL-8 (10 ng/ml) evaluated in neutrophils and LDGs from *P. vivax*-infected patients (n = 5) and neutrophils from HDs (n = 4). Data are presented as mean ± SD.

(C) Density plots (top) and bar graph (bottom) of neutrophils (n = 4) and LDGs (n = 3) from *P. vivax*-infected patients and neutrophils from HDs (n = 3) cocultured for 1 hr with purified PvRETs or uRBCs stained with CFSE (neutrophil or LDG:PvRET or uRBC ratio, 2:1). The numbers within each box refer to the cell frequencies within each gate. Data are represented as mean ± SEM. *p < 0.05, **p < 0.01.
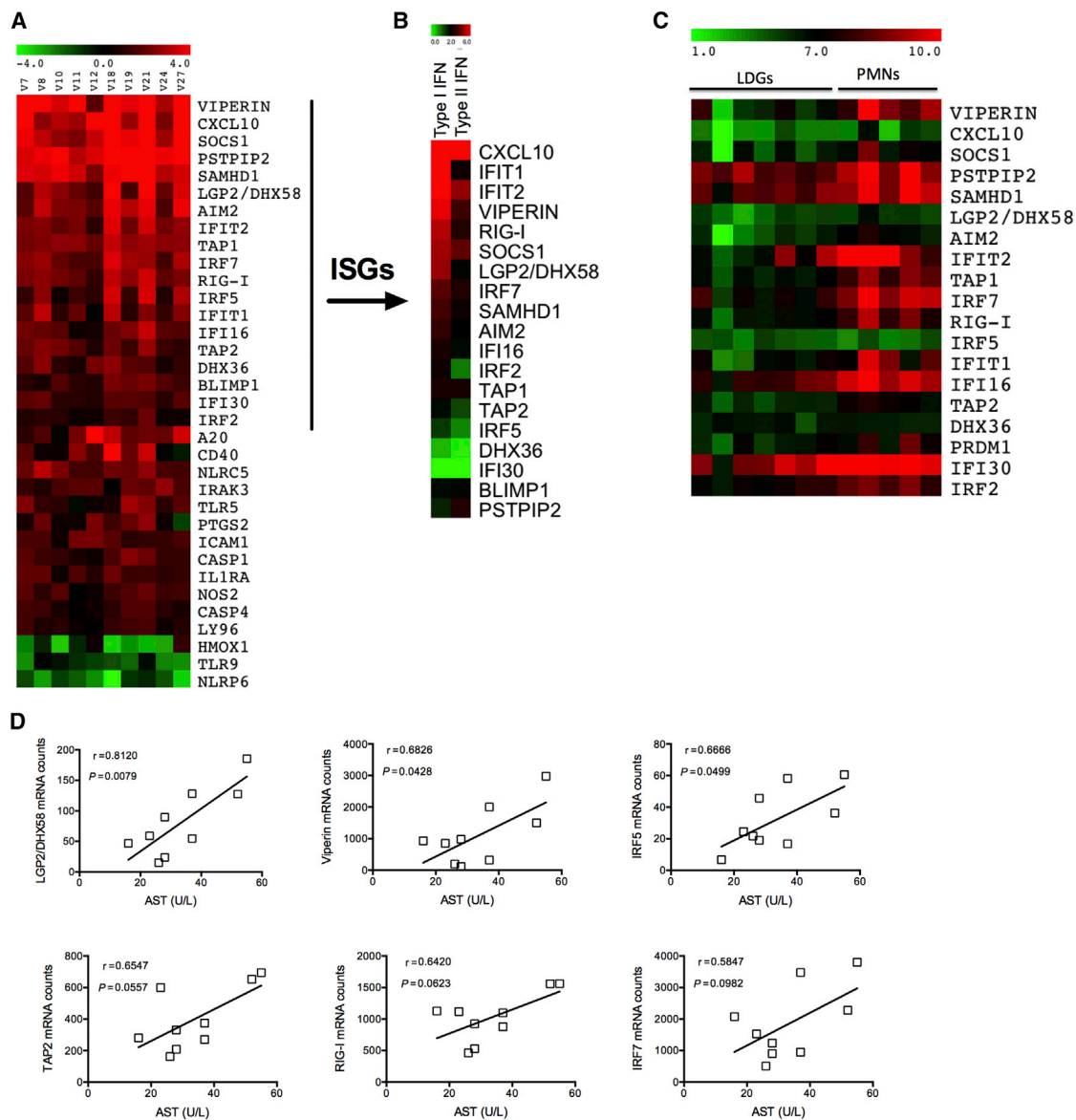
Figure 4. Neutrophils Have an IFN Transcriptional Signature during Malaria Infection

(A) Nanostring analysis of purified neutrophils from ten patients with acute *P. vivax* infections before and after treatment. Shown is a heatmap representation of 32 differentially regulated genes upon malaria infection. The heatmap shows normalized $\log_2$ ratios (*P. vivax*/after treatment) of differentially expressed genes (rows) for each patient (columns).

(B) Heatmap representation of a selection of ISGs that were significantly inducible during malaria infection. Neutrophils from healthy donors were stimulated with type I IFN (1000 U/ml) or IFN-γ (100 ng/ml) for 2 hr, and their gene expression was normalized to unstimulated cells (n = 3). The heatmap shows normalized $\log_2$ ratios (type I IFN or IFN-γ/unstimulated) of differentially expressed ISGs.

(C) mRNA counts normalized to seven housekeeping genes of LDGs (n = 7) and neutrophils (n = 5) from *P. vivax*-infected patients. Shown is a heatmap of ISGs that were differentially regulated upon malaria infection.

(D) *LGP2/DHX58*, *VIPERIN*, *IRF5*, *TAP2*, *RIG-I*, and *IRF7* mRNA counts from the nanostring analysis show a trend to correlate with AST serum levels from *P. vivax*-infected patients. The results are expressed as scatterplots of individual values. Squares indicate individual patients (n = 9). Pearson's rank correlation (r) and p values are shown in the graphs.

See also Figure S4 and Table S1.

non-infected (NI) mice, whereas the mean of infected animals increased to 177.9 ± 22.93, 204.7 ± 11.44, and 140.9 ± 3.99 neutrophils per 10× field of view (FOV) after 7, 11, and 14 days, respectively (Figure 5B). The serum ALT levels were measured

in infected animals on different days and compared with the levels of NI mice. We noticed that mice after 7, 11, and 14 days of *P. chabaudi* infection had significantly higher levels of ALT than NI mice (Figure 5C). Because we observed the
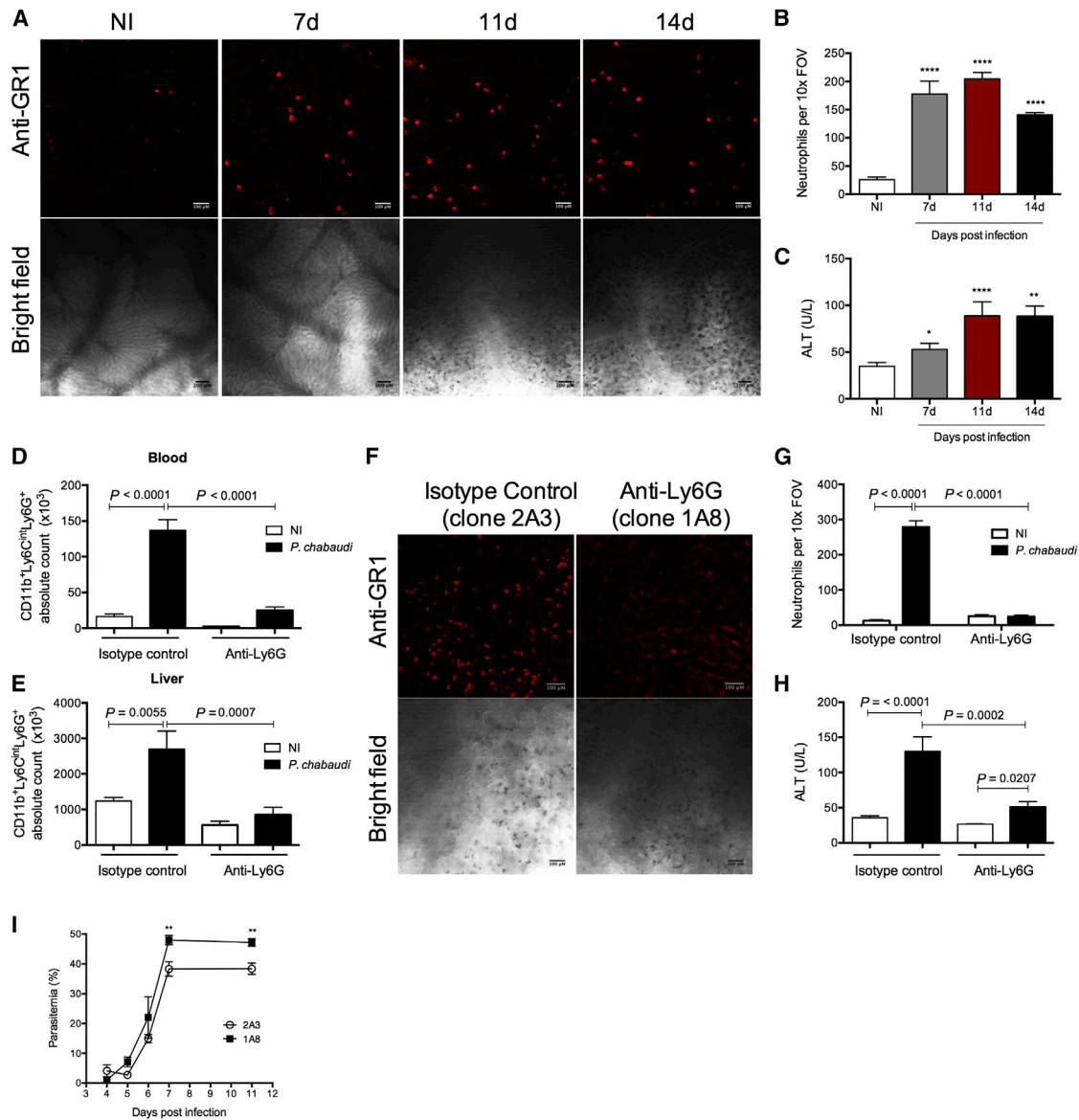
Figure 5. Following *P. chabaudi* Infection, Neutrophils Are Recruited to the Liver and Induce Liver Damage

Cells were quantified by confocal intravital microscopy.

(A) Representative images of bright-field (bottom) and neutrophil staining with anti-GR1 (top) in liver sinusoids from NI and *P. chabaudi*-infected mice from different days of infection (days 7, 11, and 14). Scale bars, 100 μM (top) and 200 μM (bottom).

(B) Absolute numbers of GR1-positive cells from at least four fields of view. The results are representative of two independent experiments (n = 4). ****p < 0.0001. Data are represented as mean ± SEM.

(C) Serum ALT levels were measured on different days of *P. chabaudi* infection and in non-infected mice (n = 8). The differences are relative to non-infected mice. *0.05 > p > 0.01; **0.01 > p > 0.001; ****p < 0.0001. Data are represented as mean ± SEM.

(D and E) Absolute neutrophil (CD11b$^+$Ly6C^{int}Ly6G$^+$) quantification by flow cytometry in peripheral blood (n = 8) (D) and in liver leukocytes (n = 5) (E) of NI and *P. chabaudi*-infected mice treated with anti-Ly6G (clone 1A8) or with an isotype control (clone 2A3). The data are relative from two independent experiments. Data are represented as mean ± SEM.

(F) Representative images of Liver intravital microscopy of the neutrophil depletion experiment after 11 days of *P. chabaudi* infection. Cells were stained with anti-GR1 (top) in mice treated with anti-Ly6G (clone 1A8) or left untreated. Bottom: bright-field image of the liver. Scale bars, 100 μM (top) and 200 μM (bottom).

(G) Quantification of GR1-positive cells from at least four fields of view (n = 3). Data are represented as mean ± SEM.

(H) Serum ALT levels were measured after 11 days of infection in mice treated with anti-Ly6G (clone 1A8) or with an isotype control (clone 2A3) (n = 8). Data are represented as mean ± SEM.

(I) Parasitemia of *P. chabaudi*-infected mice treated with either anti-Ly6G or an isotype control was evaluated by Giemsa staining of a blood smear prepared on different days post-infection. Data are represented as mean ± SEM.

See also Figure S5 and Movie S1.

highest numbers of neutrophils as well as liver damage on day 11 after infection, we decided to use this time point for subsequent experiments.

To check whether neutrophils were responsible for the observed liver damage during *P. chabaudi* infection, we depleted them by administering the anti-Ly6G monoclonal antibody (clone 1A8) to infected and NI animals. Cells were subsequently assessed by flow cytometry. We detected an ∼86% and ∼76% reduction of CD11b$^+$Ly6C^{int}Ly6G$^+$ cell population absolute numbers in the peripheral blood and livers of infected mice treated with anti-Ly6G, respectively (Figures 5D and 5E). To confirm the specificity of neutrophil depletion, we analyzed the frequency and absolute cell number of other leukocytes in whole blood (Figure S5). We also assessed neutrophil depletion in the liver by confocal microscopy (Figure 5F). On day 11 following infection, the mean neutrophil number per 10× field was 278.9 ± 17.6 (± SEM) and 24.33 ± 4.1 in *P. chabaudi*-infected mice treated with the isotype control and anti-Ly6G, respectively. Uninfected animals showed similar neutrophil counts as infected mice treated with anti-Ly6G (isotype control, 12.9 ± 2.7; anti-Ly6G, 25.6 ± 4.2) (Figure 5G). Most importantly, serum ALT levels were reduced in *P. chabaudi*-infected mice treated with anti-Ly6G to a level that was almost that of the uninfected controls (Figure 5H). Last, neutrophil depletion resulted in a slight increase in parasitemia after 7 days of infection (Figure 5I). These data demonstrate that *P. chabaudi* infection directs neutrophil recruitment to the liver, which, in turn, induces tissue damage.

Type I IFN Signaling Drives Neutrophil Recruitment to the Liver

Because we observed a predominantly type I IFN transcriptional signature in neutrophils from *P. vivax*-infected individuals, we used type I IFN receptor knockout mice (IFNαβR$^{-/-}$) to investigate the importance of type I IFN during malaria. Using confocal microscopy, we observed a reduction of neutrophil recruitment in IFNαβR$^{-/-}$ mice after 11 days of infection (Figure 6A). Wild-type (WT) mice infected with *P. chabaudi* displayed a mean of 284.1 ± 13.4 (± SEM) neutrophils per 10× FOV, whereas the average count in IFNαβR$^{-/-}$ mice was 168.6 ± 9.7 neutrophils. As predicted, based on this reduction in neutrophil recruitment, the ALT levels were reduced significantly in IFNαβR$^{-/-}$ mice to levels that were comparable with NI animals (Figure 6A).

To confirm that type I IFNs are inducing liver cells from *P. chabaudi*-infected mice, we analyzed, by qPCR, the expression of ISGs in WT and IFNαβR$^{-/-}$ mice. We found that *IFI44*, *IRF7*, and *IFIT1* were upregulated after *P. chabaudi* infection in WT mice but not induced in IFNαβR$^{-/-}$ mice (Figure 6B). We next decided to investigate whether the reduction in neutrophil recruitment in type I IFN receptor knockouts may be accounted for by a reduction in chemokines. Total mRNA was extracted from livers of NI and infected WT and IFNαβR$^{-/-}$ mice over the course of infection (days 3, 7, and 11). The loss of type I IFN signaling resulted in a marked decrease in the expression of *CCL3*, *CXCL1*, and *IL-1β* mRNA after *P. chabaudi* infection (Figure 6C). Therefore, our data suggest that type I IFN signaling triggers liver immunopathology during *P. chabaudi* infection by inducing the expression of chemokines and *IL-1β* involved in neutrophil recruitment.

When we detected a modulation of *IL-1β* mRNA by type I IFN signaling, we used Caspase-1/11 knockout mice (Casp1/11$^{-/-}$) to study neutrophil recruitment to the liver. CD11b$^+$Ly6C^{int}Ly6G$^+$ cells and serum ALT levels were significantly lower in *P. chabaudi*-infected Casp1/11$^{-/-}$ mice (Figure 6D; Figure S6), strongly suggesting a relationship between the relative neutropenia observed in knockout (KO) mice and the concomitant hepatitis as well as the conclusion that Caspases 1 and 11 are important components of liver damage.

DISCUSSION

The overt symptoms of malaria are due to the activation of innate immune cells and subsequent systemic inflammation. Indeed, when left untreated, malaria can be life-threatening. *P. falciparum* is responsible for most cases of severe malaria, whereas *P. vivax* is a relatively benign disease. However, despite its reputation for being milder, *P. vivax* malaria is not only incapacitating but has been reported to occasionally cause severe illness with complications that include acute lung injury, respiratory distress, severe thrombocytopenia, and severe anemia (Alexandre et al., 2010; Baird, 2013). Hepatic damage has also been described in both *P. falciparum* and *P. vivax* malaria (Kochar et al., 2010; Whitten et al., 2011), but the mechanisms of how malaria induces liver injury is poorly understood.

It is the common view that liver pathology during malaria infection is associated with hemolysis of infected red blood cells and the subsequent host inflammatory response to the products released from these infected cells. In animal models, elevated production of IFN-γ and IL-12 (Yoshimoto et al., 1998) and augmented infiltration of CD1d-unrestricted natural killer T (NKT) cells were associated with liver injury (Adachi et al., 2004). The most commonly held view seems to be that malaria causes a brisk hemolysis and that leukocyte recruitment to the liver subsequently results from immune activation because of the recognition of the products of erythrocytes. In turn, there is increased mRNA expression of adhesion molecules and chemokines in liver cells (Dey et al., 2012).

Although our data concerning transaminasemia do not necessarily contradict this idea, our view is that the hepatic neutrophils are actually the cause, and not the result, of hepatic injury. Indeed, in infectious disorders, neutrophils are typically the first cells to migrate to inflammatory sites, where they fight invasive pathogens (Nathan, 2006). However, the activation of neutrophils, even when appropriate, may contribute to tissue damage during excessive inflammatory reactions (Marques et al., 2015b).

During the course of malaria, hepatitis and transaminasemia are extremely common but rarely considered to be clinically important, at least with respect to serious morbidity and mortality. However, given the systemic nature of malaria, it is likely that what can be seen on the surface of the liver by intravital microscopy is happening in other organs as well. Neutrophil-mediated injury to the vascular surface of post-capillary venules, the kidney, and other sites of importance in life-threatening malaria might, in fact, result in an enhancement of the seriousness of infection. Unfortunately, like so many other aspects of innate immunity in malaria, there is only limited evidence to support this hypothesis. For example, early neutrophil depletion prevents
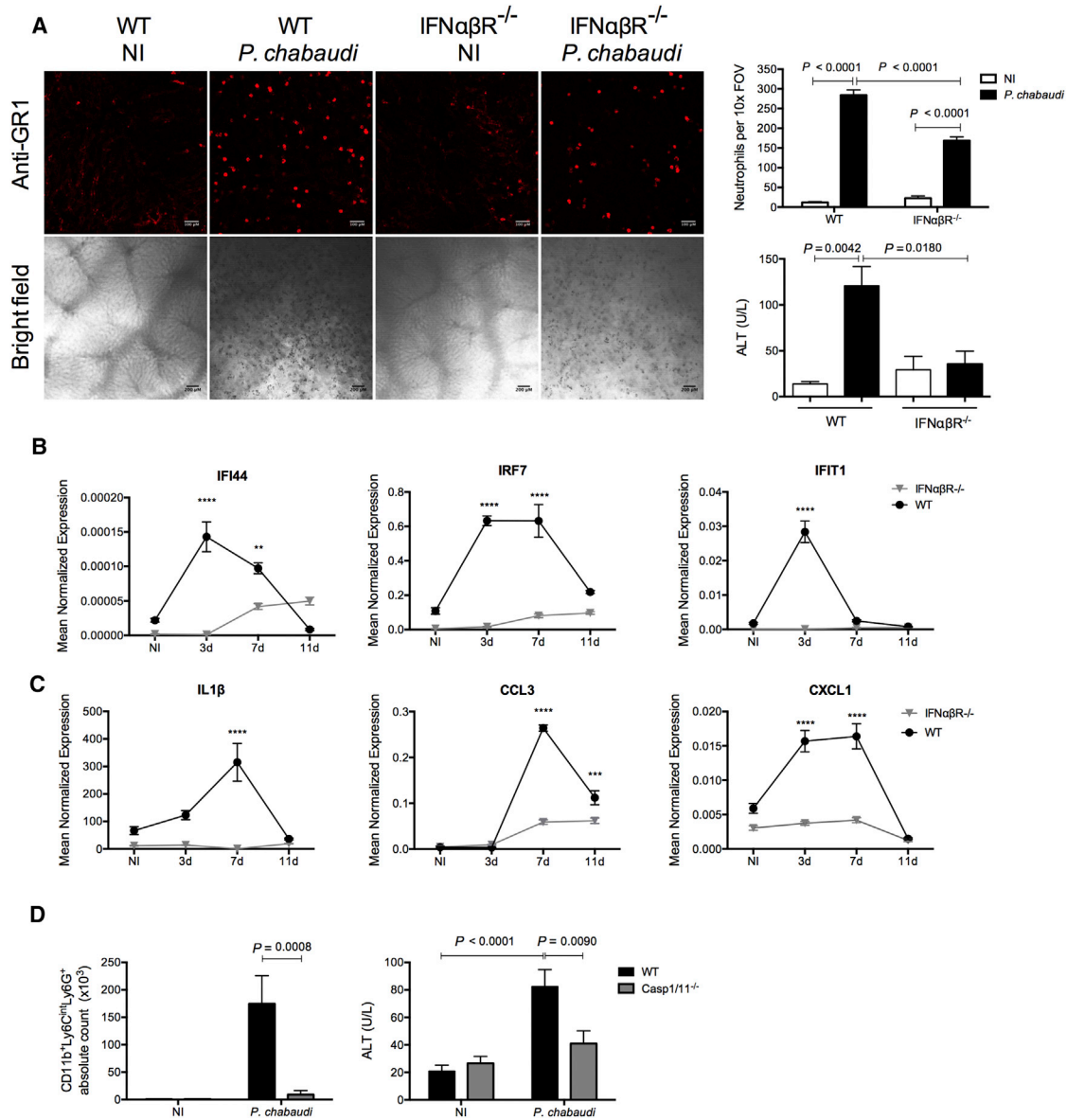
Figure 6. Type I IFN Signaling and Caspase 1/11 Function Mediate Neutrophil Recruitment to *P. chabaudi*-Infected Livers
(A) Representative images of intravital microscopy of bright-field (bottom) and neutrophil staining with anti-GR1 (top) in liver sinusoids from *P. chabaudi*-infected or non-infected WT and IFNαβR$^{-/-}$ mice. Scale bars, 100 μM (top) and 200 μM (bottom). Right: quantification of GR1-positive cells from at least four fields of view. The results are representative of two independent experiments (n = 4). Data are represented as mean ± SD (top). Serum ALT levels were measured after *P. chabaudi* infection and in non-infected WT and IFNαβR$^{-/-}$ mice (n = 4). Data are represented as mean ± SEM.
(B and C) mRNA expression of (B) the interferon-stimulated genes *IFI44*, *IRF7*, and *IFIT1* and (C) the cytokines and chemokines *IL-1β*, *CCL3*, and *CXCL1* in the livers of WT and IFNαβR$^{-/-}$ mice infected with *P. chabaudi* at different time points (3 days, 7 days, and 11 days) or left untransfected. Data are presented as a mean ± SEM of normalized expression to the GAPDH level of three biological replications. The differences are relative to WT mice. **p < 0.01, ***p < 0.001, ****p < 0.0001. See also Table S4.
(D) Absolute numbers of CD11b$^+$Ly6C^{int}Ly6G$^+$ cells (left) and serum ALT levels (right) from NI and *P. chabaudi*-infected, WT, and Casp1/11$^{-/-}$ mice. Data are represented as mean ± SEM (n = 8).
See also Figure S6.

the symptoms of cerebral malaria in mice by decreasing monocyte sequestration to the brain (Chen et al., 2000). However, this study used a monoclonal antibody (clone RB6-8C5) that also depletes dendritic cells and subpopulations of lymphocytes and monocytes (Daley et al., 2008), which makes interpretation of the results more complicated. Another tantalizing result was a report that *Plasmodium berghei* ANKA induces high-affinity immunoglobulin E receptor (FcεRI) expression in neutrophils

and that activated neutrophils migrate to the brain and mediate cerebral malaria (Porcherie et al., 2011).

An interesting observation we made is that *P. vivax* infections result in high circulating levels of activated low-density granulocytes, which is consistent with the hypothesis that neutrophils are activated during malaria. Low-density granulocytes have been reported in systemic lupus erythematosus (SLE) (Denny et al., 2010), HIV (Cloke et al., 2012), and psoriasis (Lin et al., 2011) and in certain types of cancer (Brandau et al., 2011; Rodriguez et al., 2009). The origin and activation status of LDGs are controversial because of differences found in nuclear morphology and the expression of surface markers (Brandau et al., 2011; Denny et al., 2010). Our results indicate that LDGs are mature cells based on their surface activation marker expression, once they do not express markers of neutrophil progenitors. Although the LDGs from *P. vivax*-infected patients resemble the granulocytic/neutrophilic MDSCs in terms of surface marker expression, they did not inhibit T cell proliferation (Brandau et al., 2011; Rodriguez et al., 2009). Therefore, we propose that LDGs from *P. vivax*-infected patients are highly activated degranulated neutrophils and major contributors to systemic inflammation.

We have reported previously that PBMCs have a type I IFN signature in patients with uncomplicated *P. falciparum* malaria (Sharma et al., 2011). This report expands upon that observation because we demonstrated a similar interferon signature in neutrophils during malaria. A similar pattern of gene expression has been reported in PMNs from active tuberculosis (TB) patients and correlates with disease severity, supporting a role of type I IFN in TB pathogenesis (Berry et al., 2010). The observation that ISG expression in neutrophils correlates with hepatic damage in *P. vivax* malaria patients suggests that neutrophils are migrating to the liver. Consistently, we found an enhanced expression of CCR5 and migration toward a CCL3 gradient in activated neutrophils from *P. vivax* patients.

Importantly, a high frequency of hemozoin-containing neutrophils is seen in the circulation of patients with high parasitemia and severe disease (Lyke et al., 2003). Indeed, our results suggest that neutrophils may also contribute to control parasitemia in *P. vivax*-infected patients. Therefore, we observed an augmented phagocytosis of PvRET and ROS production by neutrophils from *P. vivax* patients. These results are consistent with a study showing that neutrophils from periodontitis patients displayed an ISG signature that is associated with enhanced ROS production (Wright et al., 2008). In agreement with our results demonstrating that neutrophil depletion results in a small increase in parasitemia of mice infected with *P. chabaudi*, these studies suggest that neutrophils may play a role in resistance to human malaria.

We then decided to investigate the role of type I IFN signaling and neutrophils in a malaria experimental model. We found that type I IFN promotes neutrophil migration to the liver in *P. chabaudi*-infected mice. Consistent with this, previous reports have demonstrated that type I IFN signaling promotes leukocyte recruitment to the liver during the pre-erythrocytic stage of malaria (Liehl et al., 2014; Miller et al., 2014).

Furthermore, we found that caspase-1/11 was also necessary to mediate neutrophil recruitment to the liver. Malarial Hz has been shown to activate the NLRP3 and absent in melanoma (AIM2) inflammasome and to trigger IL-1β production (Kalantari et al., 2014; Shio et al., 2009). In addition, Hz also induces mRNA expression of several chemokines such as *CCL3*, *CCL4*, and *CXCL2* in the liver (Jaramillo et al., 2004). Taking into consideration our own results and those published elsewhere, we propose that type I IFN promotes the expression of caspase-1/11 in the liver, which generates active IL-1β, a potent inducer of chemokines that effectively recruits neutrophils.

In conclusion, our results show a pronounced expression of activation markers, transcriptional signature of ISGs, increased phagocytic activity, enhanced release of reactive oxygen species and myeloperoxidase, and high circulating levels of LDGs during *P. vivax* malaria. Although there is recent literature suggesting "innate immunity memory" or "trained immunity," this interpretation implies that this stage of augmented response to microbial stimuli is long-lasting (Quintin et al., 2014). Because neutrophils are short-lived cells and the observed effect comes to baseline (similar to HDs) after treatment, we favor the hypothesis of neutrophil priming rather than innate immunity memory or "trained immunity." Importantly, our results indicate a potential pathophysiological role for neutrophils in liver damage during malaria. Therefore, there is a need to look more closely at the role of neutrophils in the multiorgan dysfunction that accompanies truly severe disease.

EXPERIMENTAL PROCEDURES

Patients

This study was reviewed and approved by the Ethical Committees on Human Experimentation from Centro de Pesquisas em Medicina Tropical (CEP-CEPEM 096/2009), the Brazilian National Ethical Committee (CONEP 15653) of the Ministry of Health, and by the Institutional Review Board from the University of Massachusetts Medical School (IRB-ID11116_1). Patients with acute uncomplicated *P. vivax* malaria (n = 44) were enrolled based on their symptoms of fever and/or rigors in the last 24 hr before recruitment in the outpatient malaria clinic in Porto Velho (Table S2). Written informed consent was obtained before enrollment of all subjects. Up to 100 ml of peripheral blood was collected immediately after confirmation of *P. vivax* infection by a standard thick blood smear and 30–45 days after chemotherapy. Patients were treated with chloroquine and primaquine according to the Brazilian Ministry of Health, and all patients included in this study were parasitologically cured after treatment. Peripheral blood was also collected from healthy donors living in an endemic area and negative for *P. vivax* infection.

Purification of Neutrophils and Low-Density Granulocytes and Flow Cytometry Analysis

Neutrophils from *P. vivax*-infected patients before and after treatment and from HDs were isolated by Ficoll-Hypaque (GE Biosciences) gradient followed by use of a human neutrophil enrichment kit (STEMCELL Technologies) according to the manufacturer's instructions. Neutrophil purity was assessed by flow cytometry staining with the specific monoclonal antibodies listed in Table S3. LDGs were purified from PBMCs of *P. vivax*-infected patients with the CD66abce microbead kit (Miltenyi Biotec). LDGs were also analyzed by flow cytometry within PBMCs using forward scatter height (FSC-H) and SSC-H and specific monoclonal antibodies (mAbs) (Table S3). Stained cells were acquired using a FACSCan upgraded with a second laser (five colors) with Cellquest Pro and Rainbow from Cytek (BD Biosciences). Data analysis was carried out using FlowJo version 9.4.10.

Phagocytosis and Enrichment of PvRETs

Enrichment of PvRETs was performed using a 45% Percoll gradient as described previously (Carvalho et al., 2010). uRBCs were used as a negative control in the phagocytosis assay. The purity of PvRETs was determined by

optic microscopy. Purified PvRETs and uRBCs were stained with 1 μM CFSE. Purified neutrophils and LDGs from *P. vivax*-infected patients were incubated for 1 hr at 37°C, 5% CO$_2$ with purified PvRETs or uRBCs labeled previously with CFSE (neutrophil or LDG:PvRET or uRBC ratio, 2:1). The frequencies of neutrophils and LDGs positive for CFSE were determined by flow cytometry.

Chemotaxis Assay

Seventy-five thousand purified neutrophils and LDGs from *P. vivax*-infected patients and neutrophils from HDs were allowed to migrate through a 5-μm pore size, 96-well microchamber (NeuroProbe) toward CCL3 (50 ng/ml), IL-8 (CXCL8, 10 ng/ml), or medium alone. Migrated cells were counted under a light microscope.

T Cell Proliferation Assay

PBMCs from *P. vivax*-infected patients after depletion of LDGs were harvested and stained with 1 μM CFSE (Invitrogen). These cells were stimulated with soluble αCD3 (1 μg/ml) and αCD28 (0.5 μg/ml) in the presence or absence of LDGs or neutrophils (PBMC:LDG or neutrophil ratio, 2:1). After 4 days of coculture, CFSE fluorescence intensity was analyzed by FlowJo version 9.4.10. T cell proliferation was determined after gating the CD3$^+$ population and measuring the percentage of CFSE^{low} T cells.

Nanostring Analysis

Purified human neutrophils and LDGs were lysed in RLT buffer (QIAGEN) supplemented with β-mercaptoethanol and used to determine mRNA abundance by nanostring technology (Geiss et al., 2008). In brief, lysates were hybridized with the capture and reporter probes overnight at 65°C. Then they were loaded onto the nCounter prep station and quantified with the nCounter digital analyzer. For side-by-side comparisons of nCounter experiments, data were normalized with internal positive controls and with seven housekeeping genes. Finally, data from *P. vivax*-infected cells were normalized to the same cells 30–45 days after treatment. Differences in gene expression between the two conditions were considered significant when p < 0.05, as defined by multiple t test followed by the false discovery rate approach, and when the fold change was greater than 1.8. The heatmap was constructed using log$_2$-transformed data and Tiger Multi Experiment Viewer software version 4.8.

ROS Detection and MPO Quantification

For luminol-based ROS measurements, 5×10^5 neutrophils from *P. vivax*-infected patients or HDs were plated in clear-bottomed 96-well plates (Corning) in triplicate. Cells were stimulated with 100 ng/ml PMA, 2.5×10^5 PvRETs, or left untreated with medium for 2 hr in the presence of 100 μM luminol. Where indicated, the ROS production inhibitor DPI (5 μM) was added to the cell culture 30 min before stimulation. Chemiluminescence kinetics were measured by Synergy HT (BioTek Instruments) microplate reader.

One million purified neutrophils from *P. vivax*–infected individuals before and after treatment were stimulated with 100 ng/ml of PMA or left untreated for 24 hr. Supernatants were collected, and MPO levels were measured by an MPO ELISA kit (Calbiochem) according to the manufacturer's instructions.

Mice, Parasites, and Infection

C57BL/6, 129 Svev, IFNαβR$^{-/-}$, and Casp1/11$^{-/-}$ mice (8–12 weeks old) were bred and maintained under specific pathogen-free conditions in accordance with Institutional Animal Care and Use Committee (IACUC) guidelines. All protocols developed for this work were approved by the IACUC at the University of Massachusetts Medical School (ID-1369-11) and by the Council of Animal Experimentation of Oswaldo Cruz Foundation (CEUA protocol 61/13-2).

The *P. chabaudi chabaudi* AS strain was used for experimental infections. This strain was maintained in C57BL/6 mice by intraperitoneal injection of 1×10^5 infected erythrocytes (iRBCs) once a week. Parasitemia was checked every 3 days.

Quantification of Liver Neutrophils

Mouse primary nonparenchymal cells were purified from *P. chabaudi*-infected and NI mice using a 35% Percoll gradient followed by red blood cells lysis, as described before (Liehl et al., 2014). Viable nonparenchymal cells were counted by trypan blue exclusion and stained with specific mAbs (Table S3) to determine the frequency of neutrophils among liver leukocytes by flow cytometry. Stained cells were acquired using an LSRII flow cytometer (BD Biosciences). Data analysis was carried out using FlowJo version 9.4.10.

P. chabaudi-infected and NI mice were also used for confocal intravital microscopy neutrophil quantification as described previously (Marques et al., 2015a). Phycoerythrin (PE)-conjugated anti-GR1 (4 μg/mouse, 40 μg/ml, eBioscience) was injected intravenously (i.v.) 10 min before imaging. Images were obtained using a C2 Eclipse Ti confocal microscope. Neutrophil counts were performed using ImageJ software.

Neutrophil Depletion and ALT Measurement

In vivo neutrophil depletion was performed by administering four intraperitoneal (i.p.) injections of anti-Ly6G antibody (500 μg/dose, clone 1A8, BioXCell) or an isotype control (500 μg/dose, clone 2A3, BioXCell): 1 day before *P. chabaudi* infection and 2, 6, and 10 days after infection. Serum ALT activity was performed using a kinetic test (Bioclin).

qRT-PCR Analysis

Total RNA from livers of non-infected (control), 3 day-, 7 day-, or 11 day-infected mice were isolated by TRIzol reagent (Invitrogen). Quantitative PCR was carried out with the Platinum SYBR Green protocol (Invitrogen) on an Applied Biosystems 7500 real-time PCR system using the primers listed in Table S4. Relative quantification was performed using standard curve analysis, and the expression data were presented as the mean of normalized expression to the *GAPDH* level of three biological replications.

Statistical Analysis

Statistical analysis was performed using GraphPad Prism 6 software. The results were analyzed using two-tailed paired t test and one-way ANOVA between the groups. Mann-Whitney (MW) test was used when the data did not fit a Gaussian distribution. The data shown are representative of at least two independent experiments. Differences were considered to be statistically significant when p ≤ 0.05.

SUPPLEMENTAL INFORMATION

Supplemental Information includes six figures, four tables, and one movie and can be found with this article online at http://dx.doi.org/10.1016/j.celrep.2015.11.055.

REFERENCES

Adachi, K., Tsutsui, H., Seki, E., Nakano, H., Takeda, K., Okumura, K., Van Kaer, L., and Nakanishi, K. (2004). Contribution of CD1d-unrestricted hepatic DX5+ NKT cells to liver injury in Plasmodium berghei-parasitized erythrocyte-injected mice. Int. Immunol. *16*, 787–798.

Alexandre, M.A., Ferreira, C.O., Siqueira, A.M., Magalhães, B.L., Mourão, M.P.G., Lacerda, M.V., and Alecrim, Md. (2010). Severe Plasmodium vivax malaria, Brazilian Amazon. Emerg. Infect. Dis. *16*, 1611–1614.

Antonelli, L.R.V., Gigliotti Rothfuchs, A., Gonçalves, R., Roffê, E., Cheever, A.W., Bafica, A., Salazar, A.M., Feng, C.G., and Sher, A. (2010). Intranasal Poly-IC treatment exacerbates tuberculosis in mice through the pulmonary recruitment of a pathogen-permissive monocyte/macrophage population. J. Clin. Invest. *120*, 1674–1682.

Aucan, C., Walley, A.J.A., Hennig, B.J.W.B., Fitness, J., Frodsham, A., Zhang, L., Kwiatkowski, D., and Hill, A.V.S.A. (2003). Interferon-alpha receptor-1 (IFNAR1) variants are associated with protection against cerebral malaria in the Gambia. Genes Immun. *4*, 275–282.

Baird, J.K. (2013). Evidence and implications of mortality associated with acute Plasmodium vivax malaria. Clin. Microbiol. Rev. *26*, 36–57.

Berry, M.P.R., Graham, C.M., McNab, F.W., Xu, Z., Bloch, S.A.A., Oni, T., Wilkinson, K.A., Banchereau, R., Skinner, J., Wilkinson, R.J., et al. (2010). An interferon-inducible neutrophil-driven blood transcriptional signature in human tuberculosis. Nature *466*, 973–977.

Brandau, S., Trellakis, S., Bruderek, K., Schmaltz, D., Steller, G., Elian, M., Suttmann, H., Schenck, M., Welling, J., Zabel, P., and Lang, S. (2011). Myeloid-derived suppressor cells in the peripheral blood of cancer patients contain a subset of immature neutrophils with impaired migratory properties. J. Leukoc. Biol. *89*, 311–317.

Carvalho, B.O., Lopes, S.C.P., Nogueira, P.A., Orlandi, P.P., Bargieri, D.Y., Blanco, Y.C., Mamoni, R., Leite, J.A., Rodrigues, M.M., Soares, I.S., et al. (2010). On the cytoadhesion of Plasmodium vivax-infected erythrocytes. J. Infect. Dis. *202*, 638–647.

Chen, L., Zhang, Z., and Sendo, F. (2000). Neutrophils play a critical role in the pathogenesis of experimental cerebral malaria. Clin. Exp. Immunol. *120*, 125–133.

Cloke, T., Munder, M., Taylor, G., Müller, I., and Kropf, P. (2012). Characterization of a novel population of low-density granulocytes associated with disease severity in HIV-1 infection. PLoS ONE *7*, e48939.

Cunnington, A.J., Njie, M., Correa, S., Takem, E.N., Riley, E.M., and Walther, M. (2012). Prolonged neutrophil dysfunction after Plasmodium falciparum malaria is related to hemolysis and heme oxygenase-1 induction. J. Immunol. *189*, 5336–5346.

Daley, J.M., Thomay, A.A., Connolly, M.D., Reichner, J.S., and Albina, J.E. (2008). Use of Ly6G-specific monoclonal antibody to deplete neutrophils in mice. J. Leukoc. Biol. *83*, 64–70.

Denny, M.F., Yalavarthi, S., Zhao, W., Thacker, S.G., Anderson, M., Sandy, A.R., McCune, W.J., and Kaplan, M.J. (2010). A distinct subset of proinflammatory neutrophils isolated from patients with systemic lupus erythematosus induces vascular damage and synthesizes type I IFNs. J. Immunol. *184*, 3284–3297.

Dey, S., Bindu, S., Goyal, M., Pal, C., Alam, A., Iqbal, M.S., Kumar, R., Sarkar, S., and Bandyopadhyay, U. (2012). Impact of intravascular hemolysis in malaria on liver dysfunction: involvement of hepatic free heme overload, NF-κB activation, and neutrophil infiltration. J. Biol. Chem. *287*, 26630–26646.

Gazzinelli, R.T., Kalantari, P., Fitzgerald, K.A., and Golenbock, D.T. (2014). Innate sensing of malaria parasites. Nat. Rev. Immunol. *14*, 744–757.

Geiss, G.K.G., Bumgarner, R.E.R., Birditt, B., Dahl, T., Dowidar, N., Dunaway, D.L.D., Fell, H.P.H., Ferree, S., George, R.D.R., Grogan, T., et al. (2008). Direct multiplexed measurement of gene expression with color-coded probe pairs. Nat. Biotechnol. *26*, 317–325.

Haque, A., Best, S.E., Amante, F.H., Ammerdorffer, A., de Labastida, F., Pereira, T., Ramm, G.A., and Engwerda, C.R. (2011). High parasite burdens cause liver damage in mice following Plasmodium berghei ANKA infection independently of CD8(+) T cell-mediated immune pathology. Infect. Immun. *79*, 1882–1888.

Haque, A., Best, S.E., Montes de Oca, M., James, K.R., Ammerdorffer, A., Edwards, C.L., de Labastida Rivera, F., Amante, F.H., Bunn, P.T., Sheel, M., et al. (2014). Type I IFN signaling in CD8- DCs impairs Th1-dependent malaria immunity. J. Clin. Invest. *124*, 2483–2496.

Jaramillo, M., Plante, I., Ouellet, N., Vandal, K., Tessier, P.A., and Olivier, M. (2004). Hemozoin-inducible proinflammatory events in vivo: potential role in malaria infection. J. Immunol. *172*, 3101–3110.

Kalantari, P., DeOliveira, R.B., Chan, J., Corbett, Y., Rathinam, V., Stutz, A., Latz, E., Gazzinelli, R.T., Golenbock, D.T., and Fitzgerald, K.A. (2014). Dual engagement of the NLRP3 and AIM2 inflammasomes by plasmodium-derived hemozoin and DNA during malaria. Cell Rep. *6*, 196–210.

Kochar, D.K., Tanwar, G.S., Khatri, P.C., Kochar, S.K., Sengar, G.S., Gupta, A., Kochar, A., Middha, S., Acharya, J., Saxena, V., et al. (2010). Clinical features of children hospitalized with malaria–a study from Bikaner, northwest India. Am. J. Trop. Med. Hyg. *83*, 981–989.

Krücken, J., Delić, D., Pauen, H., Wojtalla, A., El-Khadragy, M., Dkhil, M.A., Mossmann, H., and Wunderlich, F. (2009). Augmented particle trapping and attenuated inflammation in the liver by protective vaccination against Plasmodium chabaudi malaria. Malar. J. *8*, 54.

Leoratti, F.M., Trevelin, S.C., Cunha, F.Q., Rocha, B.C., Costa, P.A., Gravina, H.D., Tada, M.S., Pereira, D.B., Golenbock, D.T., Antonelli, L.R., et al. (2012). Neutrophil paralysis in Plasmodium vivax malaria. PLoS Negl. Trop. Dis. *6*, e1710.

Liehl, P., Zuzarte-Luís, V., Chan, J., Zillinger, T., Baptista, F., Carapau, D., Konert, M., Hanson, K.K., Carret, C., Lassnig, C., et al. (2014). Host-cell sensors for Plasmodium activate innate immunity against liver-stage infection. Nat. Med. *20*, 47–53.

Lin, A.M., Rubin, C.J., Khandpur, R., Wang, J.Y., Riblett, M., Yalavarthi, S., Villanueva, E.C., Shah, P., Kaplan, M.J., and Bruce, A.T. (2011). Mast cells and neutrophils release IL-17 through extracellular trap formation in psoriasis. J. Immunol. *187*, 490–500.

Lyke, K.E., Diallo, D.A., Dicko, A., Kone, A., Coulibaly, D., Guindo, A., Cissoko, Y., Sangare, L., Coulibaly, S., Dakouo, B., et al. (2003). Association of intraleukocytic Plasmodium falciparum malaria pigment with disease severity, clinical manifestations, and prognosis in severe malaria. Am. J. Trop. Med. Hyg. *69*, 253–259.

Mantovani, A., Cassatella, M.A., Costantini, C., and Jaillon, S. (2011). Neutrophils in the activation and regulation of innate and adaptive immunity. Nat. Rev. Immunol. *11*, 519–531.

Marques, P.E., Antunes, M.M., David, B.A., Pereira, R.V., Teixeira, M.M., and Menezes, G.B. (2015a). Imaging liver biology in vivo using conventional confocal microscopy. Nat. Protoc. *10*, 258–268.

Marques, P.E., Oliveira, A.G., Pereira, R.V., David, B.A., Gomides, L.F., Saraiva, A.M., Pires, D.A., Novaes, J.T., Patricio, D.O., Cisalpino, D., et al. (2015b). Hepatic DNA deposition drives drug-induced liver injury and inflammation in mice. Hepatology *61*, 348–360.

Miller, J.L., Sack, B.K., Baldwin, M., Vaughan, A.M., and Kappe, S.H.I. (2014). Interferon-mediated innate immune responses against malaria parasite liver stages. Cell Rep. *7*, 436–447.

Mueller, I., Galinski, M.R., Baird, J.K., Carlton, J.M., Kochar, D.K., Alonso, P.L., and del Portillo, H.A. (2009). Key gaps in the knowledge of Plasmodium vivax, a neglected human malaria parasite. Lancet Infect. Dis. *9*, 555–566.

Murthi, P., Kalionis, B., Ghabrial, H., Dunlop, M.E., Smallwood, R.A., and Sewell, R.B. (2006). Kupffer cell function during the erythocytic stage of malaria. J. Gastroenterol. Hepatol. *21*, 313–318.

Nathan, C. (2006). Neutrophils and immunity: challenges and opportunities. Nat. Rev. Immunol. *6*, 173–182.

von der Ohe, M., Altstaedt, J., Gross, U., and Rink, L. (2001). Human neutrophils produce macrophage inhibitory protein-1β but not type I interferons in response to viral stimulation. J. Interferon Cytokine Res. *21*, 241–247.

Porcherie, A., Mathieu, C., Peronet, R., Schneider, E., Claver, J., Commere, P.H., Kiefer-Biasizzo, H., Karasuyama, H., Milon, G., Dy, M., et al. (2011). Critical role of the neutrophil-associated high-affinity receptor for IgE in the pathogenesis of experimental cerebral malaria. J. Exp. Med. *208*, 2225–2236.

Prudêncio, M., Rodriguez, A., and Mota, M.M. (2006). The silent path to thousands of merozoites: the Plasmodium liver stage. Nat. Rev. Microbiol. *4*, 849–856.

Quintin, J., Cheng, S.-C., van der Meer, J.W.M., and Netea, M.G. (2014). Innate immune memory: towards a better understanding of host defense mechanisms. Curr. Opin. Immunol. *29*, 1–7.

Rodriguez, P.C., Ernstoff, M.S., Hernandez, C., Atkins, M., Zabaleta, J., Sierra, R., and Ochoa, A.C. (2009). Arginase I-producing myeloid-derived suppressor cells in renal cell carcinoma are a subpopulation of activated granulocytes. Cancer Res. *69*, 1553–1560.

Salazar-Mather, T.P., Lewis, C.A., and Biron, C.A. (2002). Type I interferons regulate inflammatory cell trafficking and macrophage inflammatory protein 1alpha delivery to the liver. J. Clin. Invest. *110*, 321–330.

Seo, S.-U., Kwon, H.-J., Ko, H.-J., Byun, Y.-H., Seong, B.L., Uematsu, S., Akira, S., and Kweon, M.-N. (2011). Type I interferon signaling regulates Ly6C(hi) monocytes and neutrophils during acute viral pneumonia in mice. PLoS Pathog. *7*, e1001304.

Sharma, S., DeOliveira, R.B., Kalantari, P., Parroche, P., Goutagny, N., Jiang, Z., Chan, J., Bartholomeu, D.C., Lauw, F., Hall, J.P., et al. (2011). Innate immune recognition of an AT-rich stem-loop DNA motif in the Plasmodium falciparum genome. Immunity *35*, 194–207.

Shio, M.T., Eisenbarth, S.C., Savaria, M., Vinet, A.F., Bellemare, M.J., Harder, K.W., Sutterwala, F.S., Bohle, D.S., Descoteaux, A., Flavell, R.A., and Olivier,

M. (2009). Malarial hemozoin activates the NLRP3 inflammasome through Lyn and Syk kinases. PLoS Pathog. *5*, e1000559.

Sturm, A., Amino, R., van de Sand, C., Regen, T., Retzlaff, S., Rennenberg, A., Krueger, A., Pollok, J.-M., Menard, R., and Heussler, V.T. (2006). Manipulation of host hepatocytes by the malaria parasite for delivery into liver sinusoids. Science *313*, 1287–1290.

Swiecki, M., Wang, Y., Vermi, W., Gilfillan, S., Schreiber, R.D., and Colonna, M. (2011). Type I interferon negatively controls plasmacytoid dendritic cell numbers in vivo. J. Exp. Med. *208*, 2367–2374.

Whitten, R., Milner, D.A., Jr., Yeh, M.M., Kamiza, S., Molyneux, M.E., and Taylor, T.E. (2011). Liver pathology in Malawian children with fatal encephalopathy. Hum. Pathol. *42*, 1230–1239.

World Health Organization (2014). World Malaria Report 2014.

Wright, H.J., Matthews, J.B., Chapple, I.L.C., Ling-Mountford, N., and Cooper, P.R. (2008). Periodontitis associates with a type 1 IFN signature in peripheral blood neutrophils. J. Immunol. *181*, 5775–5784.

Xin, L., Vargas-Inchaustegui, D.A., Raimer, S.S., Kelly, B.C., Hu, J., Zhu, L., Sun, J., and Soong, L. (2010). Type I IFN receptor regulates neutrophil functions and innate immunity to Leishmania parasites. J. Immunol. *184*, 7047–7056.

Yamaguchi, T., Handa, K., Shimizu, Y., Abo, T., and Kumagai, K. (1977). Target cells for interferon production in human leukocytes stimulated by sendai virus. J. Immunol. *118*, 1931–1935.

Yoshimoto, T., Takahama, Y., Wang, C.R., Yoneto, T., Waki, S., and Nariuchi, H. (1998). A pathogenic role of IL-12 in blood-stage murine malaria lethal strain Plasmodium berghei NK65 infection. J. Immunol. *160*, 5500–5505.